A Fast Estimation of Initial Rotor Position for Low-Speed Free-Running IPMSM

Wu, Ting; Luo, Derong; Huang, Sheng; Wu, Xuan; Liu, Kan; Lu, Kaiyuan; Peng, Xiaoyan

Published in:
IEEE Transactions on Power Electronics

DOI (link to publication from Publisher):
10.1109/TPEL.2019.2958101

Publication date:
2020

Document Version
Accepted author manuscript, peer reviewed version

IEEE POWER ELECTRONICS REGULAR PAPER

A Fast Estimation of Initial Rotor Position for Low Speed Free-Running IPMSM

Ting Wu, Derong Luo, Sheng Huang, Xuan Wu, Kan Liu, *Senior Member*, *IEEE*, Kaiyuan Lu, *Member*, *IEEE*, *and* Xiaoyan Peng

***Abstract*—Fast and reliable initial rotor position detection is essential for re-starting sensorless permanent magnet synchronous motors (PMSMs) in free-running condition. In this paper, a fast initial rotor position estimation method for low speed free-running motor is proposed, which utilizes a combined sinusoidal current and square-wave voltage injection method. The sinusoidal current is imposed into the estimated *d*-axis to magnify magnetic saturation effect. The amplitudes of *d*-axis current caused by injected square-wave voltage are then accumulated. The large difference of the two integrated signals for positive and negative d-axes currents can be reliably used to identify the rotor polarity. Meanwhile, in low-speed free running stage, the change of saturation degrees introduced by the injected sinusoidal signal does not affect the position estimation accuracy. Moreover, even if the sinusoidal current signal is injected in the incorrect *d*-axis, the resultant torque is small and unexpected rotation of the rotor is prevented. Its influence on the free-running motor is negligible, due to the combined injection with continuously online updated estimated rotor position by high frequency (HF) square-wave voltage injection during the polarity identification process. Finally, the effectiveness of the proposed method is investigated on a 1.5 kW interior PMSM (IPMSM) test platform.**

***Index Terms*—High frequency square-wave voltage injection, initial rotor position estimation, magnetic polarity detection, permanent magnet synchronous motors (PMSMs), sensorless.**

I. Introduction

PERMANENT magnet synchronous motors (PMSMs) have an extensive use in the industrial application, featuring excellent characteristics such as high efficiency, and high power density [1-3]. For the field-oriented control (FOC) of the sensorless drive, accurate and fast estimation for initial rotor position is necessary and beneficial for reliable start-up of PMSMs [4]. The rotor alignment by using DC phase currents will cause rotor rotation, which is unacceptable in many demanding applications such as elevators, electric vehicles and draw benches, etc [5]. Therefore, the initial position of PMSM sensorless drive at zero-speed is estimated directly by exploiting the spatial signal in the PMSM. A broad variety of voltage injection methods exciting the spatial signal have been well studied, such as rotating sinusoidal voltage injection [6-8], pulsating voltage vector injection [9-10], and square-wave voltage injection [11-12]. The rotating sinusoidal voltage and pulsating voltage vector is superimposed into the stationary and the rotary frame, respectively, to excite the position-dependent high frequency (HF) current response. However, the two methods have limited the dynamic behavior due to the utilization of digital filters [13]. The square-wave voltage injection method removes the low pass filter (LPF), becomes a good choice for position estimation in the zero- or low-speed sensorless control of PMSMs [14-15]. However, there are two cycles of the machine saliency in a single electrical period, the angle ambiguity of π of the position information obtained by the above saliency-based methods cannot be differentiated. Thus, the rotor polarity identification is needed to be addressed. Various types of methods have been employed, which is generally based on saturation effect, such as short pulses injection [16-17] and secondary harmonics-based method [18-19].

The initial position estimation method at zero-speed is already a mature technology in main stream product. However, there are relatively a few researches on the initial position detection at free running condition. When the inverter is suffering from a short-term power interruption and shuts down, it takes some time for the free running motor to stop due to the energy stored in the inertia [20]. However, a suddenly re-starting of the inverter may cause overvoltage or overcurrent faults for a sensorless drive, due to mismatched terminal voltage and back-EMF [21]. This is unacceptable for the electrical drive systems in some practical applications (e.g. transportation, industrial automation, etc), which experiences frequent turn-off and on operation conditions [27]. Thus, it is of great importance to estimate the initial position of a free-running sensorless drive.

The existing algorithms for motor position estimation in a free-running condition may be roughly classified into three categories: frequency searching-based methods [22-23], back electromotive force (back-emf) based methods [24-26], and DC current injection-based methods [27]. However, the above methods are suitable for high speed free-running motor. In these methods, the performance deterioration of the back-emf based methods occurs during low-speed range due to low back-emf and stator resistance variation. The frequency searching-based

Manuscript received July 17, 2019; revised September 3, 2019; accepted November 27, 2019. This work was supported in part by the National Key Research and Development Program of China under Grant 2018YFF0212903 and in part by the National Natural Science Foundation of China under Grant 51707062, Grant 51575167 and Grant 51877075. (*Corresponding author: Derong Luo*.)

Ting Wu, Derong Luo, Xuan Wu are with the College of Electrical and Information Engineering at Hunan University, Hunan, China (e-mail: wting_tata@hnu.edu.cn; hdldr@sina.com; wuxuan24@163.com). K. Liu and X. Peng are with the College of Mechanical and Vehicle Engineering, Hunan University, Changsha 410006, China (e-mail: lkan@hnu.edu.cn; xypeng@hnu.edu.cn). S. Huang is with the Department of Electrical Engineering, Technical University of Denmark, Kongens Lyngby 2800, Denmark (e-mail: huang98123@163.com). K. Lu is with the Department of Energy Technology, Aalborg University, Aalborg 9100, Denmark (e-mail: klu@et.aau.dk).

This article has been accepted for publication in a future issue of this journal, but has not been fully edited. Content may change prior to final publication. Citation information: DOI 10.1109/TPEL.2019.2958101, IEEE Transactions on Power Electronics

methods are quite time-consuming for initial position estimation [23]; DC current injection-based methods are very promising, where the rotational direction and the speed are estimated from the *q*-axis current frequency. However, it takes longer time when the rotor speed is relatively low. However, there is quite few research work on the initial position detection at low-speed free running condition. A few fast position detection methods suitable for low speed free-running conditions have been introduced in [10],[18]. The work proposed in [18] uses the secondary harmonics of zero-sequence voltage to determine the rotor position. This method shows improvement in the position estimation performance since it is insensitive to signal processing delays, and has faster convergence than the amplitude variation based methods in [10]. However, it requires additional voltage sensing circuit to determine the zero sequence carrier voltage. The signal-to-noise ratio (SNR) of short pulses based method are superior to the methods in [10],[18]. However, the short pulses injection method is not suitable for a free-running motor, because it is implemented only when the rotor position estimation process suspends.

For solving these problems, a fast initial position detection method at low-speed free running condition together with the polarity identification is proposed. In this paper, the square-wave voltage injection method for position estimation integrates with sinusoidal AC current injection for rotor polarity detection. The polarity is determined by injecting a low-frequency sinusoidal current into estimated *d*-axis, which enlarges magnetic saturation effect. During the positive- and negative-half periods of the sinusoidal signal, the amplitude of the *d*-axis HF current induced by square-wave voltage is accumulated separately. By comparing the large difference of the two integrated value, the N/S pole is easy to be distinguished. The analysis of the change of saturation degrees caused by injected sinusoidal current signal on the position estimation accuracy and the influence of sinusoidal signal on the rotation of the motor are given in this paper. Finally, the comparative experiments with the secondary zero sequence voltage harmonics (SZSV) based method [18] is performed to prove the effectiveness of the proposed method. All experiments are carried on a 1.5-kW interior PMSM (IPMSM) drive platform.

II. Square-Wave Voltage Injection Method for Initial Position Estimations

The IPMSM can be modeled in the *dq* reference frame as follows

$$\begin{bmatrix} v_d \\ v_q \end{bmatrix} = R_s \begin{bmatrix} i_d \\ i_q \end{bmatrix} + \begin{bmatrix} L_d & 0 \\ 0 & L_q \end{bmatrix} \frac{d}{dt} \begin{bmatrix} i_d \\ i_q \end{bmatrix} + \omega_r \begin{bmatrix} 0 & -L_q \\ L_d & 0 \end{bmatrix} \begin{bmatrix} i_d \\ i_q \end{bmatrix} + \begin{bmatrix} 0 \\ \omega_r \lambda_{\mathrm{mpm}} \end{bmatrix} \tag{1}$$

where v_d, v_q, i_d, i_q, ω_r and R_s are the stator *d*-axis and *q*-axis voltages and currents, the rotor speed and the stator resistance, respectively. L_d and L_q are the *d*- and *q*-axis inductances. d/dt represents the differential operator, λ_{mpm} is the peak value of the rotor PM flux linkage.

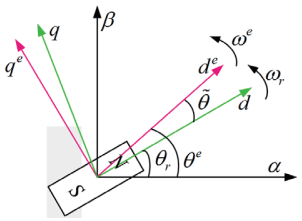

Fig.1. Coordinate distribution of each axis.

The relationship between estimated *d*-*q* reference frame (also noted as d^e - q^e reference frame) and actual *d*-*q* reference frame is illustrated in Fig.1. The square-wave voltage signal v_{inj}^e in the estimated *dq* reference frame can be described as

$$v_{inj}^e = \begin{bmatrix} v_{dh}^e \\ v_{qh}^e \end{bmatrix} = \begin{bmatrix} \pm V_{inj} \\ 0 \end{bmatrix} \tag{2}$$

where the subscript 'h' is originated from the term of 'high frequency'.

The relevant current variation induced by square-wave voltage signal v_{inj}^e in the estimated *d*-axis can be expressed as[14]

$$\begin{bmatrix} \Delta i_{dh}^e \\ \Delta i_{qh}^e \end{bmatrix} = \frac{\pm \Delta T \cdot V_{inj}}{L_1^2 - L_2^2} \begin{bmatrix} L_1 - L_2 \cos 2\tilde{\theta} \\ -L_2 \sin 2\tilde{\theta} \end{bmatrix} \tag{3}$$

where Δi_{dh}^e is the difference of peak-to-peak value of *d*-axis current, $L_1=(L_d+L_q)/2$ is the average inductance, and $L_1=(L_d-L_q)/2$ is the differential inductance. ΔT denotes the half period of square-wave voltage injection, $\tilde{\theta}$ is the position estimation error defined as $\tilde{\theta} = \theta^e - \theta_r$, θ^e is the estimated rotor position, and θ_r is the actual rotor position.

The relationship between square-wave voltage injection and PWM carrier waveform in the estimated *dq* reference frame is illustrated in Fig.2, where the injected frequency equals to the half of PWM carrier frequency. Also, to obtain the rotor position, Δi_{qh}^e in (3) that contains the position error information can be processed with an observer.

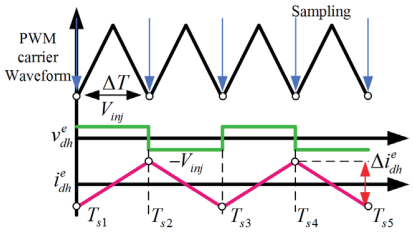

Fig.2. Implementation of square-wave voltage injection method.

III. Proposed Initial Position Estimation Method for Sensorless Control of IPMSMs

This section describes the proposed initial position estimation method suitable for low-speed free running condition. As is illustrated in Fig.3, the square-wave voltage injection is adopted to estimate the rotor position, then a sinusoidal current signal is injected into the estimated *d*-axis for magnetic polarity detection. The rotor position is continuously online updated by the HF square-wave voltage injection during the entire polarity identification process. For initial position estimation of the

This article has been accepted for publication in a future issue of this journal, but has not been fully edited. Content may change prior to final publication. Citation information: DOI 10.1109/TPEL.2019.2958101, IEEE Transactions on Power Electronics

IPMSM, the sinusoidal current injection is only performed once. In the following of two sections, the processing of the proposed method has been detailed.

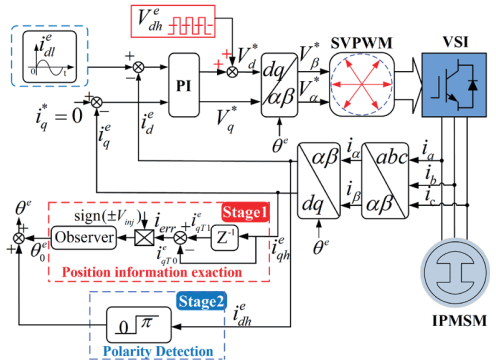

Fig.3. Proposed initial rotor position estimation method suitable for low-speed free running motor.

A. Proposed Magnet Polarity Identification Based on Sinusoidal Current Injection

Presuming that the estimated *d*-axis is consistent with the actual *d*-axis, then the position estimation error $\tilde{\theta}$ is approximately zero, the magnitude of Δi_{dh}^{e} in (3) can be derived as

$$\begin{cases} \Delta i_{dh}^{e} = \dfrac{\pm \Delta T \cdot V_{inj}}{L_1^2 - L_2^2}\left(L_1 - L_2 \cos 2\tilde{\theta}\right) \approx \dfrac{\pm \Delta T \cdot V_{inj}}{L_{dh}^{'}} \\ I_{dh}^{e} = \left|\Delta i_{dh}^{e}\right| \end{cases} \tag{4}$$

where $L_{dh}^{'}$ is the equivalent d^e-axis incremental inductance, and I_{dh}^{e} denotes the amplitude of the HF response current.

The identification of rotor magnetic polarity is achieved by imposing a sinusoidal current of i_{dl}^{e} with angular frequency $\omega_s = 2\pi f_s$ on the d^e -axis. As can be seen in (4), the amplitude of I_{dh}^{e} is inversely proportional to the incremental inductance $L_{dh}^{'}$, by injecting the current i_{dl}^{e} with angular frequency $\omega_s = 2\pi f_s$, the magnitude of I_{dh}^{e} will change with the magnetic saturation, whereas $L_{dh}^{'}$ is possible to change that is determined by the saturation condition.

The *d*-axis inductance waveform in the estimated frame [5] is illustrated in Fig.4(a), when the stator coil is imposed with a large current i_d^e, meanwhile, the rotor position is also at N pole, then the direction of the generated winding flux λ_d, is identical to that of the rotor flux λ_f. Thus, as shown in Fig.4 (b), the total stator flux $(\lambda_f + \lambda_d)$ is increased so that the stator teeth are forced to saturate further, which results in the decrease of L_d^e. By contrast, when the rotor position is at S pole, the stator teeth will be in a linear area and the value of L_d^e is maintained at its normal value. The peak values of the response current of *d*-axis under different estimated position are measured and presented as Fig.5, where a 30 V voltage with 0.5 ms added on the positive *d*-axis. It is found that the peak value of the response current is the smallest at 90°and 270°, and it is the largest when the rotor position is 0°and 180°; moreover, the current peak at 0° is slightly larger than that at 180°. The characteristics of saliency and magnetic saturation of the IPMSM are illustrated, which can be adopted to achieve the magnet polarity detection.

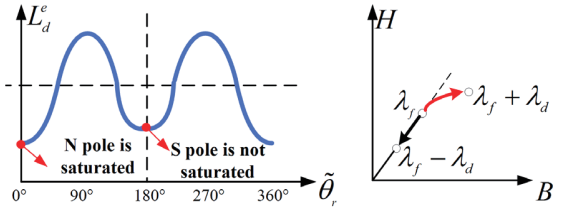

Fig.4. Principle of magnetic saturation. (a) Illustration of inductance waveform. (b) Variation of stator flux when a large current is imposed on.

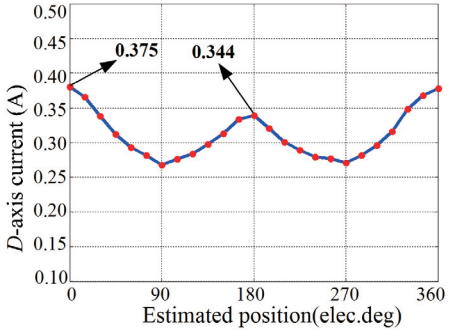

Fig.5. Relationship between the peak values of the *d*-axis current and the estimated position by adding a 30 V voltage with 5 ms on *d*-axis.

Fig.6 and Fig.7 show the HF *d*-axis current induced by square-wave voltage when the additional low-frequency sinusoidal current signal i_{dl}^{e} is applied in the estimated *d*-axis. The frequency of triangular carrier is much higher than that of sinusoidal wave. In Fig.6, when the rotor position is at N pole, the HF current response i_{dh}^{e} at T_{s2} and T_{s3} are increased, because the total stator flux under positive-half cycle of i_{dl}^{e} is augmented. However, the total stator flux under negative-half cycle of $i_{dl}^{e}$is subtracted, then the current i_{dh}^{e} at T_{s5} and T_{s6} are equal to its normal value without the saturation effects. Thus, the amplitude of the HF current I_{dh}^{e} in the positive-half period of i_{dl}^{e} (denote as I_{dh}^{+}) is larger than that in the negative-half cycle of i_{dl}^{e} (denote as I_{dh}^{-}). By contrast, when the rotor position is at S pole, $I_{dh}^{+} < I_{dh}^{-}$, the situation is reversed as illustrated in Fig.7. Hence, for sinusoidal current injection method, it alters the *d*-axis saturation degrees and the amplitude of the HF current I_{dh}^{e} is endowed with rotor magnetic polarity information. Therefore the values of I_{dh}^{+} and I_{dh}^{-} can be advantageously used for magnet polarity detection.

For the purpose to achieve data reliability, the accumulation form of I_{dh}^{e} can be considered, i.e., ΣI_{dh}^{+} and ΣI_{dh}^{-}, which denote the accumulated amplitude of the HF *d*-axis response current under the positive- and negative-cycle of the injected sinusoidal current signal. Thus, the sinusoidal current injection method can guarantee a good robustness of magnetic polarity identification for IPMSM.

This article has been accepted for publication in a future issue of this journal, but has not been fully edited. Content may change prior to final publication. Citation information: DOI 10.1109/TPEL.2019.2958101, IEEE Transactions on Power Electronics

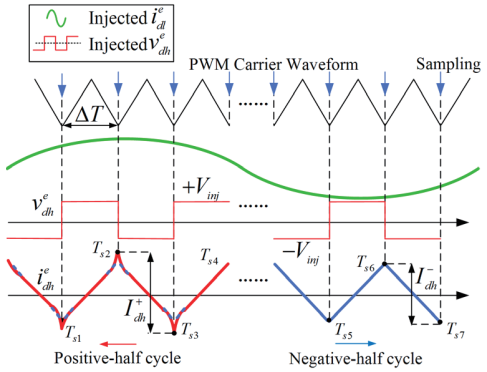

Fig.6. Resultant HF current response when the rotor is at N pole.

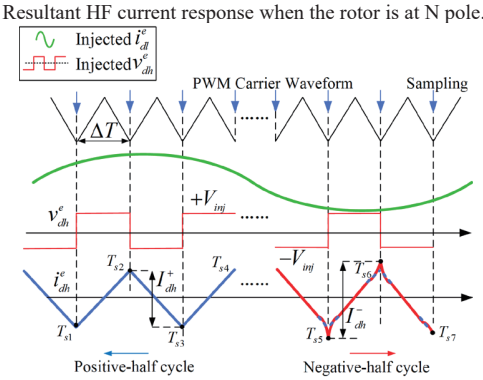

Fig.7. Resultant HF current response when the rotor is at S pole.

B. Frequency and Amplitude Selection of Sinusoidal Current Signal

The differences between I^+_{dh} and I^-_{dh} can reflect the saturation level of machine stator. Thus, the reliability of this method for magnetic polarity detection can be evaluated by the desired-to-undesired signal ratio (DUR), which is defined as

$$k_{DUR} = \frac{I^+_{dh} - I^-_{dh}}{\min\left\{I^+_{dh}, I^-_{dh}\right\}} \tag{5}$$

A HF square-wave voltage with v_{inj} =85V is applied to the *d*-axis, meanwhile, the standard DC d^e-axis current is injected from 0 to 1 p.u. In such a case, the values of $L^{'}_{dh}$ and I^e_{dh} of IPMSM are measured in Fig.8, where the spline fitted curves are drawn based on the measured data points. It is found that in Fig.8 (b), the value of K_{DUR} is higher with the increasing of the amplitude of i^e_{dl} . Considering the rated current, the injected amplitude of the sinusoidal current signal can be maximized for the improved rotor polarity detection. For the selection of sinusoidal current frequency, due to the limitation to the bandwidth of current regulator, by decreasing injection frequency below the bandwidth of current regulator, it will have a better DUR performance.

IV. Experimental Results

The proposed method is implemented on a drive with 1.5 kW IPMSM, which is illustrated in Fig.9. The variations of inductances with respect to the *dq*-axis current magnitudes using the finite-element method are shown in Fig.10, and the key

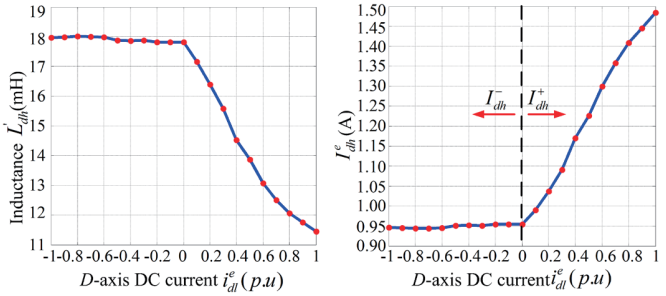

Fig.8. Effects of combination HF square-wave voltage with DC *d*-axis current in the IPMSM. (a) Measured equivalent *d*-axis incremental inductance $L^{'}_{dh}$. (b) Measured values of I^e_{dh} .

TABLE. I
IPMSM DRIVE SYSTEM PARAMETERS

Characteristics	Values	Characteristics	Values
Rated Power /kW	1.5	*q*-axis inductance/mH	26.72
Rated voltage /V	380	Number of pole pairs	2
Rated current /A	2.7	Current Sampling Freq/kHz	5
Rated speed /(r/min)	3000	PWM Switching Freq/kHz	5
d-axis Inductance /mH	17.81		

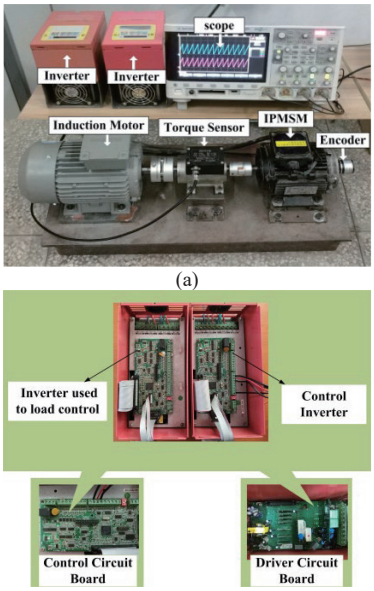

Fig.9. Experiment test setup of 1.5 kW IPMSM drive.

parameters of IPMSM are listed in Table.I. In the experiment, the proposed algorithm is implemented through a 32-bit TM320F2808 DSP. Also, the injected square-wave voltage signal has amplitude of 85V at 2.5kHz. A mechanically coupled load induction motor is employed to produce the load torque. The actual rotor position and speed are measured by an incremental encoder PENON-K3808G; these information is used to compare with the estimated position and speed, and it does not participate in the closed-loop control.

A. Verification of the Proposed Initial Position Estimation Method

Fig.11 and Fig.12 show the experimental results of proposed

This article has been accepted for publication in a future issue of this journal, but has not been fully edited. Content may change prior to final publication. Citation information: DOI 10.1109/TPEL.2019.2958101, IEEE Transactions on Power Electronics

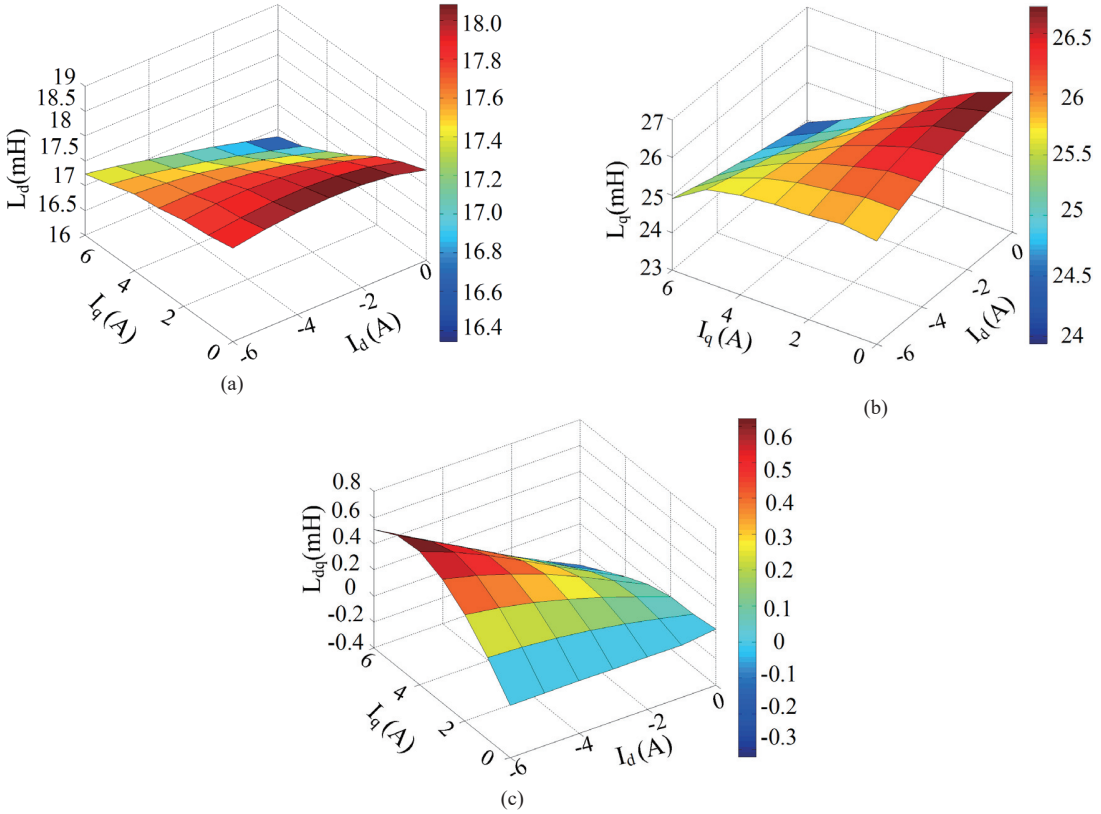

Fig.10. Inductances variation with respect to the *dq*-axis current magnitudes. (a) Variation of *d*-axis self-inductance L_d.(b) Variation of *q*-axis self-inductance L_q. (c). Variation of cross-coupling inductance L_{dq}.

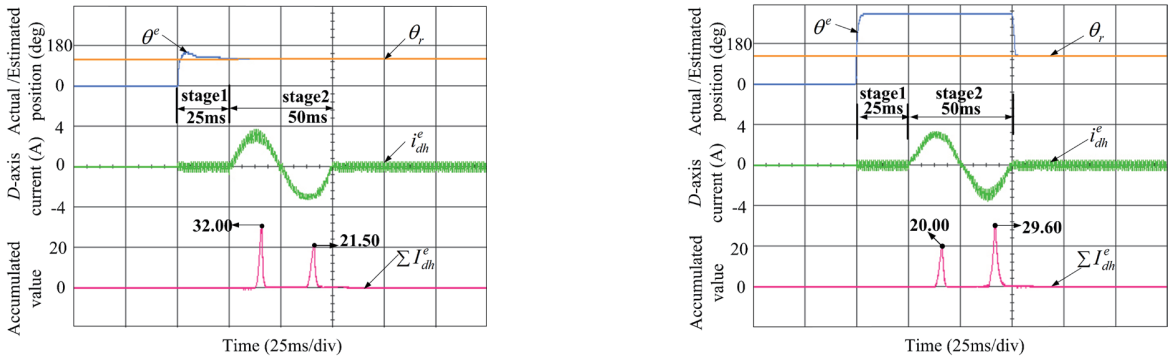

Fig.11. Initial rotor position detection in standstill situation. (a) When the rotor position is at N pole. (b) When the rotor position is at S pole.

initial position estimation method. The magnitude and frequency of i_{dl}^e is selected to be 3A (0.8p.u) and 20Hz, respectively. It takes 75 ms for obtaining the initial rotor position successfully.

In Fig.11, the IPMSM operates at standstill situation, where the rotor position is initially located at $\theta_r = 120^\circ$. As shown in Fig.11(a), firstly, the rotor position was estimated by HF square-wave voltage injection method with 25 ms, and a sinusoidal current signal is imposed on *d*-axis at stage1. At stage2, the magnetic polarity information can be obtained from the amplitude of the HF current I_{dh}^e, by accumulating the values of the positive- and the negative-half cycle of I_{dh}^e for 20 times, it can be noted that $\sum_{20} I_{dh}^+ > \sum_{20} I_{dh}^-$. Therefore, the estimated rotor position is correct, otherwise, an angle of π should be added, as shown in Fig.11 (b). Moreover, the values of K_{DUR} of the proposed method in Fig.11 (a) and (b) reach 0.49 and 0.48, respectively.

Fig.12 shows the other initial position estimation situation when the IPMSM operates in free-running mode, where the rotor position of IPMSM is initially located at $\theta_r = 264^\circ$, and the induction motor is set to speed mode, making the IPMSM rotated. As can be seen, when the rotor polarity detection is

This article has been accepted for publication in a future issue of this journal, but has not been fully edited. Content may change prior to final publication. Citation information: DOI 10.1109/TPEL.2019.2958101, IEEE Transactions on Power Electronics

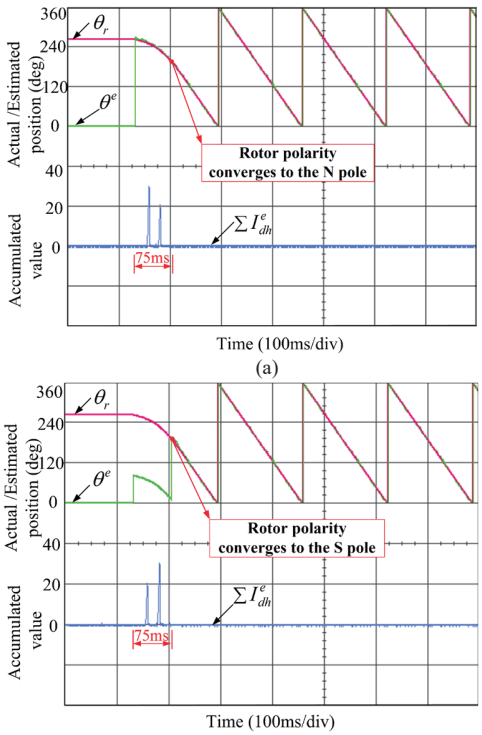

Fig.12. Initial rotor position detection in free-running mode. (a) When the rotor position is at N pole. (b) When the rotor position is at S pole.

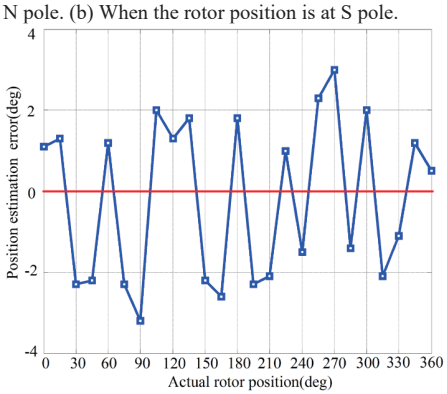

Fig.13. Position estimation error obtained by using the proposed method under different initial rotor positions.

performed, the estimated rotor position updates in real time. The whole initial rotor position estimation consumes 75ms. In Fig.12(a), no polarity correction is resulted since $\sum_{20} I_{dh}^{+} > \sum_{20} I_{dh}^{-}$. By contrast in Fig.12(b), there is $\sum_{20} I_{dh}^{+} < \sum_{20} I_{dh}^{-}$, then the correction of 180° should be added on θ^e. Therefore, the proposed initial position estimation method is a feasible approach for both standstill situation and free-running situation.

Fig.13 shows the position estimation error at different initial rotor position. The magnitude and frequency of i_{dl}^e is selected to be 3A (0.8p.u) and 20Hz respectively. The maximum and average position error is 3.2°and 1.83°, respectively. It can be seen that the proposed method gives high position accuracy.

B. Comparison

In order to verify the secondary zero sequence voltage harmonics (SZSV) based method for initial position identification [18], the rotating carrier signals are selected to be 35V/300Hz for effective magnetic polarity identification. The position tracking results of rotor and measured secondary harmonic amplitude are shown in Figs.14. As can be seen, the method has a fast position convergence taking about 30ms. Due to the secondary harmonics amplitude U_{2nd_amp} is negative, the estimated rotor direction should be compensated by π to obtain the correct position.

In addition, the SZSV based method is suitable for low speed free-running motor due to its fast response. As can be seen in Fig.15, when the estimated position has a sudden change of π in the free-running condition, the secondary harmonics of zero sequence voltage can quickly respond to track the correct rotor polarity.

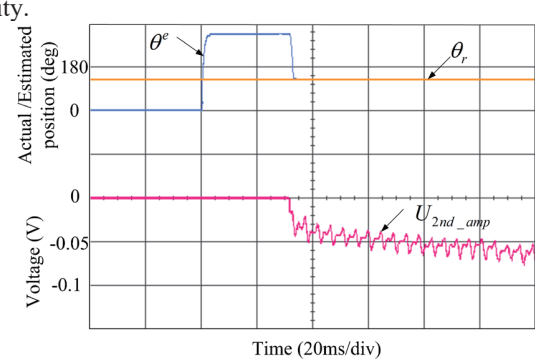

Fig.14. Magnetic polarity identification based on SZSV.

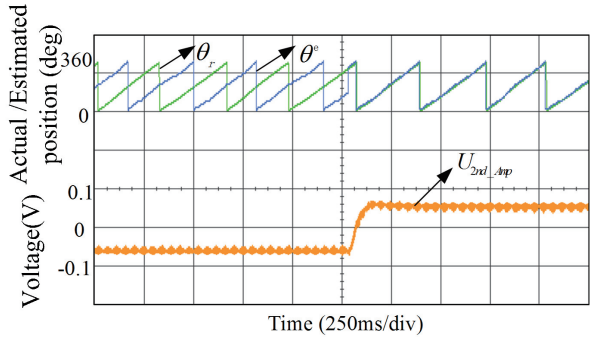

Fig.15. Secondary harmonic voltage variation due to magnetic polarity ambiguity under free-running motor.

Fig.16 illustrates the initial position estimation employing the short voltage pulses injection method for magnetic polarity detection. Usually, the longer the pulse-width is, the better the results will be, as the magnetic saturation would be more significant. However, large torque may be produced and exists there for a longer time, causing unexpected rotation of the rotor. The pulse-width is generally chosen as 5-11 times the switching period [28]. The intervals of two pulses should be long enough for the current to decay to zero. Thus, in this paper, the amplitude of short pulse is chosen to be 248V, and the two voltage pulses is with a pulse-width of 1ms and at intervals of 50 ms. As shown in Fig.16(a), the *d*-axis current induced by positive voltage pulse is higher than the current induced by negative voltage pulse, so the estimated position is not needed to

This article has been accepted for publication in a future issue of this journal, but has not been fully edited. Content may change prior to final publication. Citation information: DOI 10.1109/TPEL.2019.2958101, IEEE Transactions on Power Electronics

be corrected. Otherwise, as shown in Fig. 16(b), it needs to be added with an angle of π.

Compared to the proposed method, the short pulse injection method cannot be used for initial position detection for a low speed free-running motor. The reason is that the method cannot be applied together with the HF injection method for position estimation. The SZSV based method has faster convergence for the free-running rotor, however, it requires additional voltage sensing circuit to determine the zero-sequence carrier voltage. Moreover, its SNR is lower than the proposed method; the amplitude variation of second harmonic voltage in Fig.14 is less than 0.1V, it will be more sensitive to the potential sources of distortion than the proposed method.

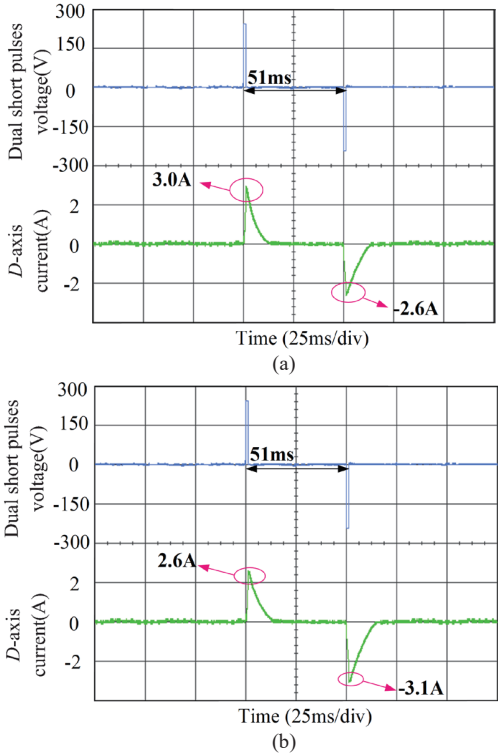

Fig.16. Applying with short pulses injection for magnetic polarity detection. (a) Current response of *d*-axis when the rotor position is at N pole. (b) Current response of *d*-axis when the rotor position is at S pole.

C. Effects of the proposed sinusoidal current injection method on the DUR

In this section, the comparison of K_{DUR} of the proposed sinusoidal current injection method under different amplitudes and frequencies is presented and their effects on the rotor polarity identification are analyzed.

Fig.17 and Fig.18 present the HF *d*-axis current with the injection of different sinusoidal current signal, where the rotor position is initially located at $\theta_r = 120^\circ$. In Fig.17 (a), the injected magnitude and frequency of i_{dl}^e is 1.9A and 50 Hz, respectively. As can be seen, the K_{DUR} is 0.293, and when the injection amplitude is increased by 2 times, as shown in Fig.17(b), the K_{DUR} reaches 0.55. In Fig.18, the injected frequency of i_{dl}^e increases to 100Hz, the magnitude is 1.9A and 3.8A, respectively. It can be observed that the value of K_{DUR} is 0.278 in Fig.18(a)，and 0.528 in Fig.18(b).

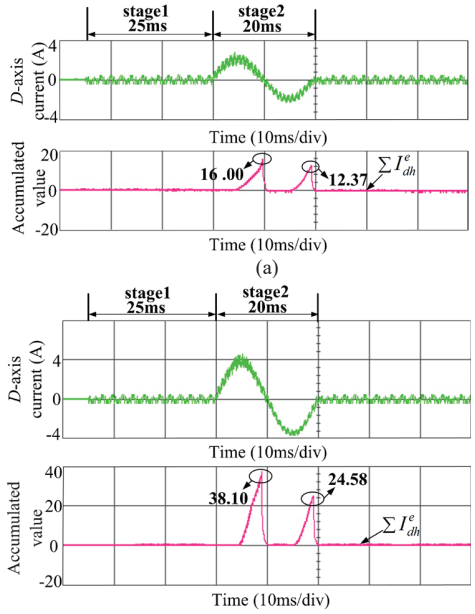

Fig.17. *D*-axis current and accumulated amplitude of the HF current response with sinusoidal current injection on the *d*-axis at standstill. (a) Sinusoidal current with 50 Hz and 1.9 A. (b) Sinusoidal current with 50 Hz and 3.8 A.

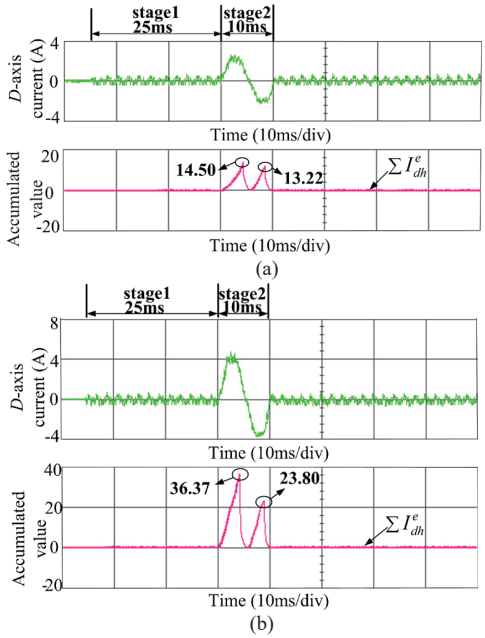

Fig.18. *D*-axis current and accumulated amplitude of the HF current response with sinusoidal current injection on the *d*-axis at standstill. (a) Sinusoidal current with 100 Hz and 1.9 A. (b) Sinusoidal current with 100 Hz and 3.8 A.

For the purpose to evaluate how the frequency and amplitude of sinusoidal current i_{dl}^e influence the magnetic polarity detection, the K_{DUR} with respect to the frequency f_s and amplitude A_s of sinusoidal current signal is illustrated in Fig.19. It can be observed that, for fixed amplitude A_s, the value of K_{DUR} reduces gradually with the change of frequency from 20 Hz to 200 Hz

This article has been accepted for publication in a future issue of this journal, but has not been fully edited. Content may change prior to final publication. Citation information: DOI 10.1109/TPEL.2019.2958101, IEEE Transactions on Power Electronics

(the bandwidth of the current controller). In the frequency from 20 Hz to 100 Hz, the decrease degree of K_{DUR} is smaller than that from 100 Hz to 200 Hz. For fixed frequency f_s, the value of K_{DUR} is increased as the amplitude A_s increases. When A_s =1p.u and f_s =20Hz, the maximum value of K_{DUR} is K_{Max} =0.57.

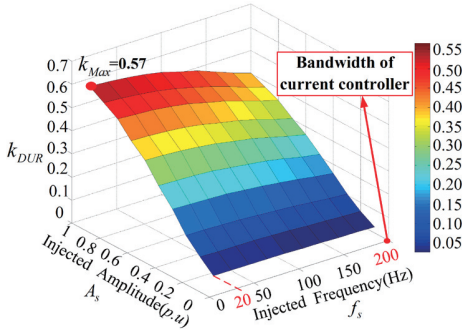

Fig.19. k_{DUR} with respect to the frequency and amplitude of the injected sinusoidal current signal.

D. *Analysis of Sinusoidal Current Injection on the rotation of motor and position estimation accuracy*

Fig.20 shows the experimental results when the IPMSM is at low-speed free-running condition, where the rotor speed is 90r/min(3Hz), the sinusoidal signal for polarity detection is selected to 1p.u (rated current). It is observed from that, during the polarity detection, the speed has little change. The reason is that the current is injected on the estimated *d*-axis, whose location is continuously updated online during the entire initial position polarity identification process by using the HF square-wave voltage injection method. The position estimation error is small; therefore, the injected current on the estimated *d*-axis will not cause noticeable position or speed variations.

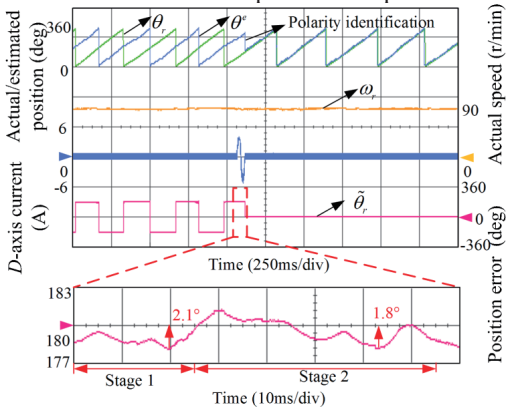

Fig.20. Experimental results of the proposed method under machine free-running conditions.

As can be seen from the zoomed view of position estimation error in Fig.20, the maximum position estimation error without the *d*-axis current injection is 2.1° ; then when adding the *d*-axis current sinusoidal injection, the maximum position estimation error is 1.8°. Therefore, the estimated position is not changed much which means the *d*-axis current will not influence the estimation accuracy. Moreover, the position estimation error caused by cross-saturation effects is more strongly influenced by the *q*-axis current than the d-axis current. Especially for a motor with high *d*-axis saturation degree, it is much less affected by cross-saturation effects [29].

E. *Sensorless performance of the proposed method*

The experimental results of position sensorless control under rated step load of IPMSM are shown in Fig. 21. As can be seen, the speed fluctuates at the moments when step load is imposed and removed. Its recovery time is about 0.5s. During the whole process, the position error is within 18° . Therefore, the proposed position estimation method has a good robustness performance in step load condition.

Moreover, the Bode plot was used for evaluating the performance of the speed controller and position observer. The bandwidth can be considered as the frequency where 45 degs phase delay occurs in the Bode plot. Fig. 22 shows the Bode diagram of the speed controller and position observer, respectively. The PI parameters of the speed loop are K_{Pw}=0.68 and τ= 0.0029; the PI parameters of the Phase-locked loop (PLL) are k_{pt}= 75.40 and k_{it}= 56.85. As can be seen, the bandwidth of the speed loop and the position observer is 28.8 Hz and 11.9 Hz, respectively.

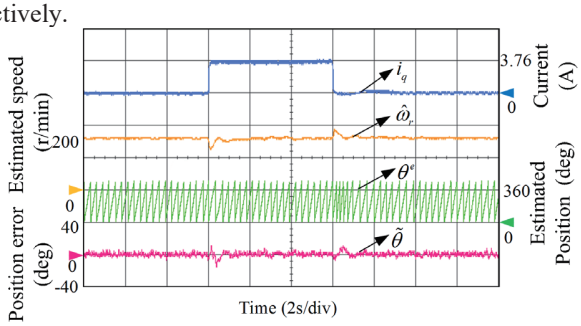

Fig.21. Speed control performance under rated step load at 200r/min.

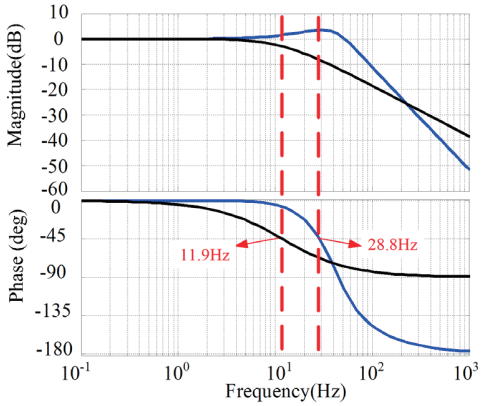

Fig. 22. Bode diagram of the speed loop and the position observer.

For assessing the performance of the whole sensorless startup process, the experimental results under different loads are illustrated in Fig.23. In the experiment, the rotor position is initially located at $\theta_r = 144^\circ$, and the speed is increasing from 0 r/min to 200 r/min. The process can be divided into three stages. Firstly, the stage is quiescent period and the drive is not started. The second stage is in the start-up period. The initial rotor

This article has been accepted for publication in a future issue of this journal, but has not been fully edited. Content may change prior to final publication. Citation information: DOI 10.1109/TPEL.2019.2958101, IEEE Transactions on Power Electronics

position can be successfully obtained within 75 ms during T1 stage, during the polarity identification process about 50 ms, the rotor location is continuously updated online by using the HF square-wave voltage injection method. Then during the T2 period, the *q*-axis current starts to rise up, and the starting torque is also increased suddenly so that the motor starts to rotate in the T3 stage, where the *q*-axis current trends to increase, until the motor reached the appointed speed. Finally, when the motor operates at a steady state, the *q*-axis current is smaller than that in the T3 stage, the IPMSM system has entered a steady state. After the motor starts up with 150% rated load, the position estimation error is within 10°.

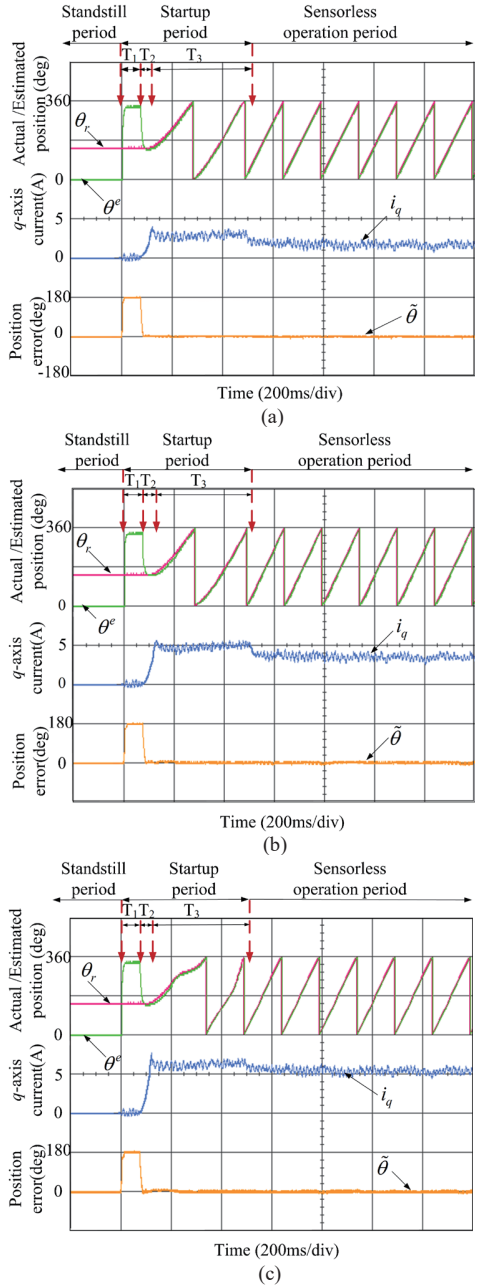

Fig.23. Process from standstill to steady running of IPMSM under different load. (a)With 50% rated load. (b)With 100% rated load. (c)With 150% rated load.

V. Conclusions

Key conclusions are summarized as follows.

1) An initial position detection method at low-speed free running condition, with fast response and good reliability is proposed. The low-frequency sinusoidal current signal is presented for rotor polarity identification. For low-speed free running motor, the change of saturation degrees resulted from sinusoidal current injection does not affect the position estimation accuracy.

2) During polarity identification, the influence of low-frequency sinusoidal current signal on the rotation of free-running motor is negligible, because the rotor position is continuously online updated by the high frequency (HF) square-wave voltage injection during the entire polarity identification process.

References

[1] M. J. Corley , R. D. Lorenz, "Rotor position and velocity estimation for a salient-pole permanent magnet synchronous machine at standstill and high speeds," *IEEE Trans. Ind. Appl.*, vol. 34, no. 4, pp. 784-789, Jul/Aug. 1998.

[2] G. Wang, T. Li, G. Zhang, X. Gui, and D. Xu, "Position estimation error reduction using recursive-least-square adaptive filter for model-based sensorless interior permanent-magnet synchronous motor drives," *IEEE Trans. Ind. Electron*., vol. 61, no. 9, pp. 5115–5125, Sep. 2014.

[3] M. E. Haque, Limin Zhong, M. F. Rahman, "A sensorless initial rotor position estimation scheme for a direct torque controlled interior permanent magnet synchronous motor drive," *IEEE Trans. Power Electron.*, vol. 18, no. 6, pp. 1376-1383, Nov. 2003.

[4] J. Holtz, "Acquisition of Position Error and Magnet Polarity for Sensorless Control of PM Synchronous Machines," *IEEE Trans. Ind. Appl.*,vol. 44, no. 4, pp. 1172-1180, Jul/aug. 2008.

[5] G. Wang, G. Zhang, R. Yang, D. Xu, "Robust Low-Cost Control Scheme of Direct-Drive Gearless Traction Machine for Elevators Without a Weight Transducer," *IEEE Trans. Ind. Appl*., vol. 48, no. 3, pp. 996-1005, May/Jun. 2012.

[6] T. Kikuchi, Y. Matsumoto and A. Chiba, "Fast Initial Speed Estimation for Induction Motors in the Low-Speed Range," *IEEE Trans. Ind. Appl.*, vol. 54, no. 4, pp. 3415-3425, Jul/Aug. 2018.

[7] Q. Gao, G. Asher , M. Sumner, "Sensorless Position and Speed Control of Induction Motors Using High-Frequency Injection and Without Offline Precommissioning," *IEEE Trans. Ind. Electron.*, vol.54, no.5, pp. 2474-2481, Oct. 2007.

[8] J. M. Liu, Z. Q. Zhu, "Novel Sensorless Control Strategy With Injection of High-Frequency Pulsating Carrier Signal Into Stationary Reference Frame," *IEEE Trans. Ind. Appl.*, vol. 50, no. 4, pp. 2574-2583, Jul/Aug. 2014.

[9] G. Wang, R. Yang, and D. Xu, "Dsp-based control of sensorless IPMSM drives for wide-speed-range operation," *IEEE Trans. Ind. Electron*., vol.60, no. 2, pp. 720–727, Feb. 2013.

[10] L. M. Gong and Z. Q. Zhu, "Robust Initial Rotor Position Estimation of Permanent-Magnet Brushless AC Machines With Carrier-Signal-Injection-Based Sensorless Control," *IEEE Trans. Ind. Appl*., vol. 49, no. 6, pp. 2602-2609, Nov.-Dec. 2013.

[11] G. Xie, K. Lu, S. K. Dwivedi, J. R. Rosholm and F. Blaabjerg, "Minimum-Voltage Vector Injection Method for Sensorless Control of PMSM for Low-Speed Operations," *IEEE Trans. Power Electron.*, vol. 31, no. 2, pp. 1785-1794, Feb. 2016.

[12] Q. Tang, A. Shen, X. Luo and J. Xu, "PMSM Sensorless Control by Injecting HF Pulsating Carrier Signal Into ABC Frame," *IEEE Trans. Power Electron.*,vol. 32, no. 5, pp. 3767-3776, May. 2017.

[13] Y. Yoon, S. Sul, S. Morimoto, K. Ide, "High-Bandwidth Sensorless Algorithm for AC Machines Based on Square-Wave-Type Voltage Injection," *IEEE Trans. Ind. Appl.*, vol. 47, no. 3, pp. 1361-1370, May./Jun.2011.

[14] G. Wang, D. Xiao, N. Zhao, X. Zhang, W. Wang, D. Xu, "Low-Frequency Pulse Voltage Injection Scheme-Based Sensorless Control of IPMSM

Drives for Audible Noise Reduction," *IEEE Trans. Ind. Electron.*, vol. 64, no. 11, pp. 8415-8426, Nov. 2017.
[15] S. Kim, J. Ha and S. Sul, "PWM Switching Frequency Signal Injection Sensorless Method in IPMSM," *IEEE Trans. Ind. Appl.*, vol. 48, no. 5, pp. 1576-1587, Sept/Oct. 2012.
[16] S. Li, S. Zheng, X. Zhou, J. Fang, "A Novel Initial Rotor Position Estimation Method at Standstill for Doubly Salient Permanent Magnet Motor," *IEEE Trans. Ind. Inform.*, vol. 14, no. 7, pp. 2914-2924, Jul. 2018.
[17] D. Raca, M. C. Harke and R. D. Lorenz, "Robust Magnet Polarity Estimation for Initialization of PM Synchronous Machines With Near-Zero Saliency," *IEEE Trans. Ind. Appl.*, vol. 44, no. 4, pp. 1199-1209, Jul./aug. 2008.
[18] P. Xu and Z. Q. Zhu, "Initial Rotor Position Estimation Using Zero-Sequence Carrier Voltage for Permanent-Magnet Synchronous Machines," *IEEE Trans. Ind. Electron*., vol. 64, no. 1, pp. 149-158, Jan. 2017.
[19] Yu-seok Jeong, R. D. Lorenz, T. M. Jahns, Seung-Ki Sul, "Initial rotor position estimation of an interior permanent-magnet synchronous machine using carrier-frequency injection methods," *IEEE Trans. Ind. Appl*., vol. 41, no. 1, pp. 38-45, Jan./Feb. 2005.
[20] H. Yang, Y. Zhang, P. D. Walker, J. Liang, N. Zhang, B. Xia, "Speed sensorless model predictive current control with ability to start a free running induction motor," *IET Electr. Power Appl.,* vol. 11, no. 5, pp. 893-901, May.2017.
[21] Z. You and S. Yang, "A Control Strategy for Flying-Start of Shaft Sensorless Permanent Magnet Synchronous Machine Drive," *IPEC-Niigata 2018 -ECCE Asia*, 2018, pp. 651-656.
[22] K. Lee, S. Ahmed and S. M. Lukic, "Universal Restart Strategy for Scalar (V/f) Controlled Induction Machines," *IEEE Trans. Ind. Appl*., vol. 53, no.6, pp. 5489-5495, Dec. 2017.
[23] S. Kim, H. Par, A. Yoo, H. Lee and J. Seok, "Soft-restarting of free-run induction motors driven by small DC-link capacitor inverters," *2015 IEEE Energy Conversion Congress and Exposition (ECCE), Montreal, QC,* 2015, pp. 4441-4446.
[24] L. Pravica, D. Sumina, T. Bariša, M. Kovačić and I. Čolović, "Flying Start of a Permanent Magnet Wind Power Generator Based on a Discontinuous Converter Operation Mode and a Phase-Locked Loop," *IEEE Trans. Ind. Electron*., vol. 65, no. 2, pp. 1097-1106, Feb. 2018.
[25] K. Fujinami and K. Kondo, "Linearization method for starting control of speed-sensorless vector-controlled induction motors," *IEE Japan Trans*., vol. 130-D, no. 11, pp. 1255–1263, 2010.
[26] H. Tajima, Y. Matsumoto, and H. Umida. "Speed sensorless vector control method for an industrial drive system." *IEE Japan Trans*. vol. 116, no. 11, pp. 1103-1109, 1996.
[27] H. Iura, K. Ide and T. Hanamoto, "An Estimation Method of Rotational Direction and Speed For Free-Running AC Machines without Speed and Voltage Sensor," *IEEE Trans. Ind. Appl*., vol. 47, no. 1, pp. 153-160, Feb.2011.
[28] Y. Li, H. Lu, W. Qu and S. Sheng, "An in-depth study on initial rotor position estimation of interior permanent magnet synchronous motor based on di/dt principle," *2011 International Conference on Electrical Machines and Systems, Beijing*, 2011, pp. 1-6.
[29] Z. Q. Zhu, Y. Li, D. Howe, C. M. Bingham, and D. Stone, "Influence of machine topology and cross-coupling magnetic saturation on rotor position estimation accuracy in extended back-EMF based sensorless PM brushless AC drives," *In Proc. 42nd IAS Annu. Meet*.,2007, pp. 2378- 2385."

Ting Wu was born in Hunan, China, in 1994. She received the B.S. and M.S. degree from Hunan Institute of Engineering in 2016, and from Hunan University in 2018, respectively. She is currently working toward the Ph.D. degree in College of Electrical and Information Engineering, Hunan University, Changsha, China. Her current research interests include permanent magnet synchronous motor drive and position sensorless control.

Derong Luo was born in Hunan, China, in 1968. He received the M.S. and Ph.D. degrees both in College of Electrical and Information Engineering, Hunan University, Changsha, China, in 1990 and 2003, respectively. He is currently a Professor in the College of Electrical and Information Engineering, Hunan University, Changsha, China. His research interests include permanent magnet synchronous motor drives, position sensorless control of AC motors.

Sheng Huang received the M.S. and Ph.D. degree both in College of Electrical and Information Engineering, Hunan University, Changsha, China, in 2012 and 2016, respectively. He is currently a Postdoc with the Center for Electric Power and Energy, Department of Electrical Engineering, Technical University of Denmark. His research interests include renewable energy generation, modeling and integration study of wind power, control of energy storage system, and voltage control.

Xuan Wu was born in Hunan, China, in 1983. He received the M.S. and Ph.D.degrees in Automation from the College of Electrical and Information Engineering, Hunan University, Changsha, China, in 2011 and 2016, respectively. He is an Associate researcher in the College of Electrical and Information Engineering, Hunan University. His research interests include permanent magnet synchronous motor drives, position sensorless control of AC motors.

Kan Liu (M'14-SM'17) received the B.Eng. and Ph.D. degrees in Automation from the Hunan University, China, in 2005 and 2011, respectively, and the Ph.D. degree in Electronic and Electrical Engineering from the University of Sheffield, Sheffield, U.K., in 2013. From 2013 to 2016, he was a research associate with the Department of Electronic and Electrical Engineering, the University of Sheffield. From 2016 to 2017, he was a lecturer with the Control Systems Group of the Loughborough University.
He is currently a Professor of Electro-mechanical Engineering at the Hunan University. His research interests include parameters estimation and sensorless control of permanent magnet synchronous machine drives and compensation of inverter nonlinearity, for applications ranging from automotive engineering to servo system. Prof. Liu serves as an Associate Editor for the IEEE Access, and also a Guest Editor/Associate Editor for the Journal of Control Science and Engineering, the International Journal of Rotating Machinery, and the CES Transactions on Electrical Machines and Systems. He is also the Acting Director of the Engineering Research Center of the Ministry of Education on Automotive Electronics and Control

Technology.

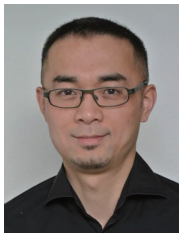

Kaiyuan Lu (M'11) received the B.S. and M.S. degrees from Zhejiang University, Zhejiang, China, in 1997 and 2000 respectively, and the Ph.D. degree from Aalborg University, Denmark, in 2005, all in electrical engineering. In 2005, he became an Assistance Professor with the Department of Energy Technology, Aalborg University, where he has been an Associate Professor since 2008. His research interests include design of permanent magnet machines, finite element method analysis, and control of permanent magnet machines.

Xiaoyan Peng received the B.S. and M.S. degrees in mechanical engineering, and the Ph.D. degree in automatic control from Hunan University, Changsha, China, in 1986, 1989, and 2013, respectively. She is currently a Professor with the College of Mechanical and Vehicle Engineering, Hunan University, Changsha, China. Her research interests include control of mechatronic systems and safety analysis of autonomous vehicles.